Eur J Nucl Med Mol Imaging (2009) 36:607–615
DOI 10.1007/s00259-008-0995-7

ORIGINAL ARTICLE

Respiration-averaged CT for attenuation correction in non-small-cell lung cancer

Nai-Ming Cheng · Chih-Teng Yu · Kung-Chu Ho · Yi-Cheng Wu · Yuan-Chang Liu · Chih-Wei Wang · Tzu-Chen Yen

Received: 10 June 2008 / Accepted: 17 October 2008 / Published online: 3 December 2008

Abstract
Purpose Breathing causes artefacts on PET/CT images. Cine CT has been used to reduce respiratory artefacts by acquiring multiple images during a single breathing cycle. The aim of this prospective study in non-small-cell lung cancer (NSCLC) patients was twofold. Firstly, we sought to compare the motion artefacts in PET/CT images attenuation-corrected with helical CT (HCT) and with averaged CT (ACT), which provides an average of cine CT images. Secondly, we wanted to evaluate the differences in maximum standardized uptake values (SUV_{max}) between HCT and ACT.
Methods Enrolled in the study were 80 patients with NSCLC. PET images attenuation-corrected with HCT (PET/HCT) and with ACT (PET/ACT) were obtained in all patients. Misregistration was evaluated by measurement of the curved photopenic area in the lower thorax of the PET images for all patients and direct measurement of misregistration for selected lesions. SUV_{max} was measured separately at the primary tumours, regional lymph nodes, and background.
Results A total of 80 patients with NSCLC were included. Significantly lower misregistrations were observed in PET/ACT images than in PET/HCT images (below-thoracic misregistration 0.25±0.58 cm vs. 1.17±1.17 cm, $p<0.001$; lesion misregistration 1.38±2.10 vs. 3.10±4.09, $p=0.013$). Significantly higher SUV_{max} were noted in PET/ACT images than in PET/HCT images in the primary tumour ($p<0.001$) and regional lymph nodes ($p<0.001$). Compared with PET/HCT images, the magnitude of SUV_{max} in PET/ACT images was higher by 0.35 for the main tumours and 0.34 for lymph nodes.
Conclusion Due to its significantly reduced misregistration, PET/ACT provided more reliable SUV_{max} and may be useful in treatment planning and monitoring the therapeutic response in patients with NSCLC.

Keywords Averaged CT · Attenuation correction · Non-small-cell lung cancer · Misregistration · Standardized uptake value

N.-M. Cheng · K.-C. Ho · T.-C. Yen (✉)
Department of Nuclear Medicine,
Chang Gung Memorial Hospital Linkou Medical Center,
5 Fu-Shih St.,
Taoyuan 333, Taiwan
e-mail: yen1110@adm.cgmh.org.tw

C.-T. Yu
Department of Chest Medicine,
Chang Gung Memorial Hospital and Chang Gung University,
Taoyuan, Taiwan

Y.-C. Wu
Department of Chest Surgery,
Chang Gung Memorial Hospital and Chang Gung University,
Taoyuan, Taiwan

Y.-C. Liu
Department of Diagnostic Radiology,
Chang Gung Memorial Hospital and Chang Gung University,
Taoyuan, Taiwan

C.-W. Wang
Department of Pathology,
Chang Gung Memorial Hospital and Chang Gung University,
Taoyuan, Taiwan

Introduction

Despite the advances in chemotherapy of non-small-cell lung cancer (NSCLC), the clinical outcome for patients with this condition remains dismal [1, 2]. It is therefore essential to predict early an insufficient response to therapy in order to save time and cost by changing early the treatment protocol and avoiding unnecessary toxic side effects while preserving survival benefits for responders.

Imaging plays a crucial role in the clinical management of NSCLC including diagnosis, staging and follow-up. Metabolic imaging with ^{18}F-FDG PET has been shown to improve accuracy in staging of NSCLC compared with traditional CT imaging [3, 4]. Interestingly, previous studies have demonstrated that FDG uptake in NSCLC correlates with tumour proliferation, pathological grade [4–8] and overall survival rates [9–12]. Assessment of therapy response by FDG-PET should be possible at earlier time points compared with anatomical imaging because changes in tumour metabolism precede a reduction in tumour size [9]. For the quantitative evaluation of regional FDG to predict treatment response, standardized uptake values (SUV) have been previously used in NSCLC [7, 13]. In this context, accurately reproducible SUV measurements are critical for reliable use in evaluation of therapy. However, respiratory motion often hampers accurate localization and quantification of PET/CT imaging in NSCLC [14–17]. The artefact is due to the discrepancy between the chest position on the CT image and the chest position on the PET image. Because of the longer acquisition time of PET scans, they are acquired while the patient is freely breathing. The final image is thus an average of many breathing cycles. On the other hand, a CT scan is usually acquired during a specific stage of the breathing cycle. This difference in respiratory motion between PET scans and CT scans causes breathing artefacts on PET/CT scans (helical CT followed by PET) [18, 19]. Cine CT acquires multiple low-dose CT images in one breathing cycle and has been successfully used to reduce respiratory artefacts. Attenuation correction of PET data with averaged CT (ACT)—that averages ten phases of cine CT images—has been proposed for improving the registration of PET and CT in thoracic cancer imaging [19–21] and cardiac imaging [22–25]. However, its effectiveness has not yet been investigated in a large-scale clinical trial.

We therefore conducted this prospective study focused on the potential clinical usefulness of ACT for attenuation correction of PET data in NSCLC. Specifically, the aims of the present study were twofold: (1) to compare the effects on motion artefacts in PET/CT data of attenuation correction with helical CT (HCT) and ACT in NSCLC, and (2) to evaluate the differences in maximum SUV (SUV_{max}) between attenuation correction with HCT (PET/HCT) and attenuation correction with ACT (PET/ACT).

Materials and methods

Patients

This study was approved by the Institutional Review Board of Chang Gung Memorial Hospital. Written informed consent was obtained from all patients. Inclusion criteria were as follows: (a) histological or cytological diagnosis of NSCLC (squamous cell carcinoma, adenocarcinoma, large-cell carcinoma); (b) age >20 years; and (c) patient with NSCLC referred either for initial staging or restaging after one or more courses of therapy. Excluded were patients with a history of synchronous malignancy, prior malignancy, pregnancy, fasting blood glucose >200 mg/dl, or unsuitable for FDG PET studies.

FDG PET/CT image acquisition

Patients were asked to fast for 6 h before examination. No intravenous contrast agent was used for enhancement in the CT scan. The studies were performed using the same PET/CT scanner (Discovery ST16, GE Healthcare) 50 min after intravenous administration of FDG. The injected dose of FDG was calculated according to the patient's body weight and ranged from 370 to 555 MBq. Attenuation corrections of PET images with HCT and ACT was performed. The helical CT data were acquired at the following settings: 120 kV, automatic mA (ranging from 10 to 300 mA), pitch 1.75:1, collimation 16×3.75 mm, and rotation cycle 0.5 s. Without changing the patient position, a whole-body PET emission scan was performed in 2-D mode from skull to mid-thigh. Following HCT and PET acquisition, a low dose-cine CT scan was performed using a "step and shoot" technique [20, 21], at the following settings: 120 kV, automatic mA (ranging from 10 to 25 mA according to the patient's body weight), rotation cycle 0.5 s, collimation 8×2.5 mm, and cine duration 5.9 s [24, 26]. Cine CT coverage was chosen to include bilateral lung fields, from the pulmonary apex to the dome of the liver. HCT and ACT acquisitions were performed with the patient in free breathing. Ten phases of cine CT images were averaged to obtain ACT for attenuation correction of the PET data [18, 20, 21]. Details of postprocessing information of ACT for PET attenuation correction have been reported by Pan et al. [22]. HCT and ACT images were rebinned from a 512×512 matrix to a 128×128 matrix and matched to the pixel size of the PET data in order to match the in-slice resolution of the PET emission images. The ACT data for the thoracic region were combined with HCT data obtained outside the thoracic area in order to generate CT images to be used for attenuation correction of the PET data. PET emission data were reconstructed using both the HCT and ACT attenuation maps. Transaxial emission images of 3.3×3.3×3.27 mm^3 (in plane matrix size 128×128, 47 slices per bed position) were reconstructed using ordered subsets expectation maximization with four iterations and ten subsets.

PET/CT data analysis and image interpretation

PET images were first assessed using transaxial, sagittal, and coronal displays for any obviously abnormal foci of

increased FDG uptake. Three experienced nuclear medicine physicians read the images, identified the lesions and performed staging according to the 2002 American Joint Committee on Cancer (AJCC), 6th edition, staging criteria. Identification of malignant lung lesions (primary tumour lesions or malignant lymph node involvement) was based on histopathological findings obtained upon completion of the study, clinical consensus or patient follow-up. Measurement of SUV_{max} and estimation of misregistration (see below) were also performed. Primary lung tumours were anatomically classified as situated in the upper, middle and lower lung lobes. Large lesions which crossed different lobes and were difficult to assign to the upper, middle and lower lobes were excluded. Lesions in regional lymph nodes were classified as situated in the superior mediastinal nodes, aortic nodes, inferior mediastinal nodes, and N1 nodes according to the mediastinal nodal station system [27]. Extrapulmonary lesions in the ACT coverage were also analysed. A lung lesion was defined as "problematic" as follows: (1) when a change in TNM staging occurred due to different lesion localizations as detected by PET/HCT and PET/ACT, and (2) when there was a discrepancy in the tissue or organ localization of lesions as detected by PET/HCT and PET/ACT. When lesions occurred at problematic localizations, independent CT or MRI scans were performed. The background area was used to test whether the use of ACT would result in an increased SUV_{max} in areas with no or limited respiratory motion. We used the aortic arch to represent the background.

Regions of interest (ROIs) were manually drawn by the same investigator on transaxial images around the areas with increased FDG uptake. SUV_{max} of lung lesions and the aortic arch were calculated for both PET/HCT and PET/ACT images using Advantage Workstation version 4.2 (GE Healthcare). Care was taken not to include regions of calcification of the aortic arch in ROIs for SUV_{max} measurement. The magnitudes of SUV_{max} changes were evaluated by the absolute difference and percentage change between PET/HCT and PET/ACT. A prominent SUV_{max} difference was defined as a change in SUV_{max} of >10% in PET/HCT and PET/ACT data.

Measurement of misregistration artefacts

Misregistration artefacts in PET scans were defined as curved photopenic areas in the lower thorax [19]. In PET scans, the distances between blank areas were bilaterally measured slice-by-slice in the anteroposterior and mediolateral directions of the coronal and sagittal views, respectively. The maximum height between blank areas was assessed by three expert nuclear medicine physicians and the results were averaged. The maximal height (in centimetres) of measured blank areas was recorded in every patient. A below-thoracic misregistration size of 1 cm or more was defined as a prominent misregistration.

The craniocaudal motions of lung lesions in NSCLC patients were directly accessed by visual estimation to determine the slice with the maximum area of lesion activity and size in the transverse images of the PET and CT scans, respectively. A similar methodology was used to access the spatial registration of PET and CT in the lung [16]. In order to identify lesions visually, three criteria were used in this study. First, the lesion had to be identifiable from the surrounding tissue in both PET and CT scan images. Second, the border of the lesion had to be clearly identified in both PET and CT scans. Third, lesions with a heterogeneous distribution of ^{18}F-FDG (such as in the presence of central necrosis) were excluded. We used a lung window (window 1,000 HU, level −700 HU) for CT, and a fixed intensity for PET. Since it was known that the pixel size was 3.27 mm for the craniocaudal axis, the distance (in millimetres) could be calculated. Subsequently, we compared the difference in the location between the CT and PET scans and this was used to indicate the misregistration. The same procedure was performed for HCT and ACT.

Statistical analysis

Continuous data are reported as means±standard deviation (SD). Differences between groups were assessed by paired two-tailed t test for continuous variables. Pearson χ^2 analysis was performed to compare the frequencies of prominent misregistration between ACT attenuation-corrected PET and HCT attenuation-corrected PET. Pearson correlation coefficients were calculated to assess the relationship between misregistration and the change in SUV_{max} (expressed as percentages). Statistical analyses were performed using SPSS (SPSS, Chicago, IL). Two-tailed p values <0.05 were considered statistically significant.

Results

Patients

Between 1 July 2007 and 31 May 2008, a total of 80 patients (42 men and 38 women; median age 66.5 years, range 34–93 years) were enrolled. A total of 80 PET/CT datasets were obtained. The clinical characteristics of the study participants are shown in Table 1. Of the 80 patients, 42 (52.5%) were referred for primary staging and 38 (47.5%) for restaging. The predominant histological type was adenocarcinoma (52.5%). The mean body weight of the patients was 57.3 kg, and their mean height was 1.60 m. The majority of patients (61.25%) were diagnosed as having advanced NSCLC. In this study, two lung lesions

Table 1 Clinicopathological characteristics of the 80 patients

Characteristic	Number of patients (%)
Sex	
Male	42 (52.5)
Female	38 (47.5)
Age (years)	
≤50	8 (10)
50–60	12 (15)
60–70	32 (40)
>70	28 (35)
Total PET scan	
Primary staging	42 (52.5)
Restaging	38 (47.5)
Tumour cell type	
Adenocarcinoma	42 (52.5)
Squamous cell carcinoma	19 (23.8)
NSCLC	17 (21.3)
Large-cell cancer	2 (2.5)
Treatment	
Surgery	34 (42.5)
Radiotherapy	34 (42.5)
Chemotherapy	62 (77.5)
Pathological stage[a]	
I	7 (8.8)
II	3 (3.8)
IIIa	21 (26.3)
IIIb	27 (33.8)
IV	22 (27.5)

[a] AJCC 2002 staging.

fitted the criteria of a "problematic" localization (Figs. 1 and 2). Follow-up CT findings and the clinical course were used to verify the diagnosis.

Magnitude and frequency of misregistration in PET/CT

The occurrence and magnitude of below-thoracic misregistration in ACT attenuation-corrected PET were significantly lower than in HCT attenuation-corrected PET. The occurrence of prominent misalignment was 55.0% in HCT attenuation-corrected PET and 12.5% in ACT attenuation-corrected PET ($p<0.001$). The mean value was 1.17± 1.17 cm in HCT attenuation-corrected PET and 0.25± 0.58 cm in ACT attenuation-corrected PET ($p<0.001$). In patients with "prominent" misregistrations in PET/HCT ($n=44$), misregistrations were entirely removed in 28 patients (63.64%) and reduced in 14 patients (31.82%) following PET/ACT. The maximum height of below-thoracic misregistration was 4.53 cm in HCT attenuation-corrected PET and 2.45 cm in ACT attenuation-corrected PET.

A total of 38 lesions were identified for direct evaluation of the misalignment between PET and CT. Of these, 17 were located in the upper, 7 in the middle, and the remaining 14 in the lower lung. Due to the use of CT scans without contrast enhancement, the possibility of identifying lymph nodes from the background soft tissue was limited. Thus we did not specifically focus on this issue in this study. Lesion misregistration was significantly less with ACT than with HCT (3.10±4.09 mm in PET/HCT vs. 1.38±2.10 mm in PET/ACT, $p=0.013$). Moreover, there was a highly significant correlation between the change in lesion misregistration and the percentage change in SUV_{max} in PET/HCT and PET/ACT ($r=0.773$, $p<0.001$). In contrast, for the selected lesions, the correlation between the change in below-thoracic misregistration and the change in SUV_{max} was not significant ($r=0.300$, $p=0.067$).

SUV_{max} in primary tumours and regional lymph nodes

Table 2 shows the ratios of SUV_{max} in HCT attenuation-corrected PET to that in ACT attenuation-corrected PET in the primary tumours and regional lymph nodes. ACT-attenuation-corrected PET showed higher SUV_{max} than HCT-attenuation-corrected PET in 87.8% of primary tumours (72/82), and in 92.7% of involved lymph nodes (115/124). SUV_{max} in ACT-attenuation-corrected PET images were significantly higher than in HCT-attenuation-corrected images both in primary tumours ($p<0.001$) and in

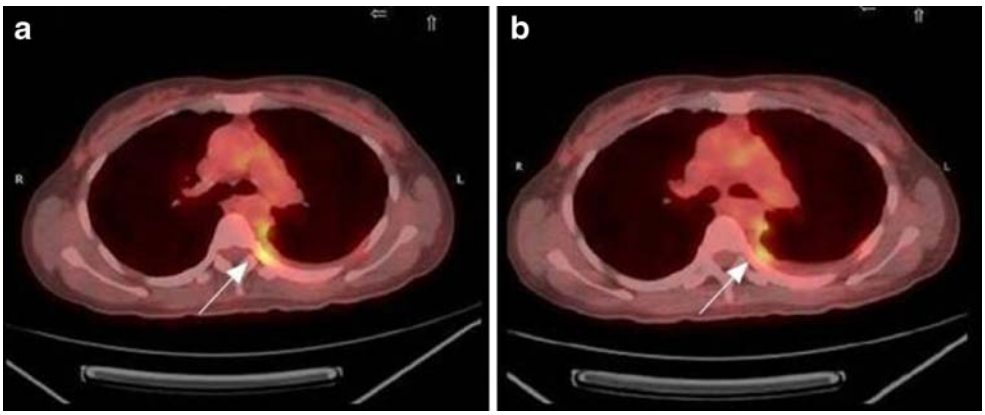

Fig. 1 Problematic localization. A 43-year-old female patient underwent a PET/CT scan for primary staging of lung adenocarcinoma of the left upper lobe. PET/HCT disclosed tumour seeding in the left pleura with left rib invasion (**a** *arrow*). Notably, PET/ACT demonstrated tumour seeding in the left pleura without left rib invasion (**b**)

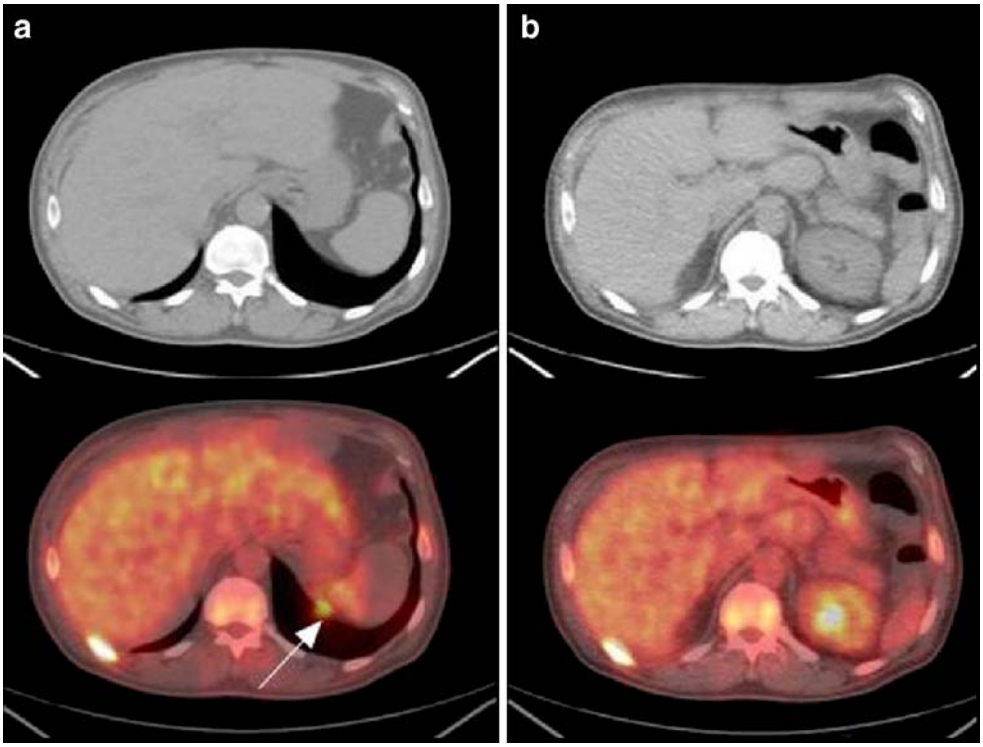

Fig. 2 Problematic localization. Attenuation correction of the same PET data by HCT (**a**) and ACT (**b**) in a 48-year-old male patient with documented NSCLC at the right upper lung. The patient underwent PET/CT for primary staging. In the PET/HCT scan (**a**), left lower pleural seeding was highly suspected (T2N0M1, stage IV; AJCC 2002). However, no corresponding lesion was evident in the ACT scan (**b**). In the PET/ACT scan, a physiological accumulation of FDG radioactivity in the kidney (T2N0M0, stage Ib) – rather than pleural seeding – was observed

regional lymph nodes ($p<0.001$; Table 3), the only exception being primary tumours located in the middle lobe of the lung ($p=0.198$). In primary tumours, the average SUV_{max} elevation in PET/ACT images was 0.35 (3.92% higher than the corresponding SUV_{max} in PET/HCT images). The primary tumours located in the lower lung field showed the higher increase in SUV_{max} (0.54, or 5.49% higher). In lymph nodes, SUV_{max} elevation was 0.34 (5.44%). The most striking SUV_{max} differences (more than 10% between PET/HCT and PET/ACT) were observed in eight primary tumours (9.76%), 25 lesions in lymph nodes (20.16%), and in one bone lesion (10%). The greatest elevation in SUV_{max} was 45.95% (7.4 in PET/HCT images, 10.8 in PET/ACT images; Fig. 4).

Table 2 Distribution of SUV_{max} in primary tumours and lymph nodes

	n	ACT/HCT SUV_{max} ratio[a]	
		≥1	<1
Primary tumours			
Total	82	72	10
Upper lung[b]	34	29	5
Middle lung[c]	14	10	4
Lower lung[d]	34	33	1
Lymph nodes			
Total	124	115	9
Superior mediastinum[e]	43	42	1
Aortic[f]	13	13	0
Inferior mediastinum[g]	22	18	4
N1[h]	46	42	4

[a] SUV_{max} in ACT-attenuation-corrected PET divided by SUV_{max} in HCT-attenuation-corrected PET.
[b] Upper lobes.
[c] Right middle and left lingula lobes.
[d] Lower lobes.
[e] Highest mediastinal, upper paratracheal, prevascular and retrotracheal, lower paratracheal lymph nodes.
[f] Aortopulmonary window and paraaortic lymph nodes.
[g] Subcarinal, paraoesophageal and pulmonary ligament lymph nodes.
[h] Hilar, interlobar, lobar, segmental and subsegmental lymph nodes.

In contrast, the difference in background activity between PET/ACT and PET/HCT was not significant ($n=80$, 2.04±0.37 in PET/HCT and 2.05±0.38 in PET/ACT, $p=0.462$).

A total of ten bone lesions were identified in our study (seven in the thoracic spine, two in the ribs, and one in the sternum). In bone lesions overall, a significant increase in SUV_{max} was evident. In the lesions in the thoracic vertebrae, no significant increase in SUV_{max} was evident (6.79±3.91 in PET/ACT vs. 6.54±3.78 in PET/HCT, $p=0.09$). This was probably due to their immobility during respiration. There were three bulky tumours extending through the interlobar fissures into the adjacent lobe. These lesions were excluded due to difficulties in assigning them to the upper, middle or lower lobes.

Discussion

FDG PET is increasingly being used to monitor the effectiveness of therapy in patients with NSCLC [4–8, 13]. Unfortunately, respiratory motion remains a major

Table 3 SUV_{max} in tumours and lymph nodes

	n	HCT (mean±SD)	ACT (mean±SD)	*p*	Absolute difference (range)	Percentage difference (range)
Main tumours						
Total	82	8.97±6.02	9.32±6.24	<0.001	0.35 (−0.80–3.40)	3.92 (−15.00–45.95)
Upper lung[a]	34	7.66±4.64	7.85±4.68	<0.001	0.19 (−0.10–0.90)	2.81 (−1.79–12.96)
Middle lung[b]	14	9.66±5.93	9.94±5.98	0.198	0.28 (−0.80–2.10)	2.78 (−15.00–22.58)
Lower lung[c]	34	10.00±7.12	10.54±7.46	<0.001	0.54 (−0.20–3.40)	5.49 (−8.70–45.95)
Lymph nodes						
Total	124	6.22±3.89	6.56±4.11	<0.001	0.34 (−0.70–2.10)	5.44 (−20.00–37.78)
Superior mediastinum[d]	43	6.37±4.23	6.79±4.47	<0.001	0.42 (−0.20–1.50)	6.75 (−5.71–27.78)
Aortic[e]	13	6.45±2.76	6.88±2.93	0.011	0.42 (0–1.70)	6.80 (0–37.78)
Inferior mediastinum[f]	22	8.22±4.78	8.49±4.86	0.002	0.27 (−0.30–1.10)	3.85 (−6.82–14.00)
N1[g]	46	5.07±2.94	5.34±3.27	<0.001	0.27 (−0.70–2.10)	4.60 (−20.00–20.00)
Bone						
Total	10	6.20±3.17	6.43±3.28	0.022	0.23 (0–0.90)	3.80 (0–11.11)
Thoracic spine	7	6.54±3.78	6.79±3.91	0.092	0.24 (0–0.90)	3.80 (0–11.11)

[a] Upper lobes.
[b] Right middle and left lingula lobes.
[c] Lower lobes.
[d] Highest mediastinal, upper paratracheal, prevascular and retrotracheal, lower paratracheal lymph nodes.
[e] Aortopulmonary window and paraaortic lymph nodes.
[f] Subcarinal, paraoesophageal and pulmonary ligament lymph nodes.
[g] Hilar, interlobar, lobar, segmental and subsegmental lymph nodes.

challenge in imaging NSCLC [18, 19]. Hence, the accuracy and reproducibility of SUV measurement is of paramount importance for correct interpretation of NSCLC status.

PET/CT is currently most commonly used in NSCLC patients in whom it has shown advantages over either PET or CT alone. However, PET/CT misregistrations occur frequently and can create artefacts, especially when the CT scan is acquired during inspiration [14–17]. In this regard, CT attenuation coefficients may be underestimated when the diaphragm is displaced from its normal location by air-filled lung tissues. Under these circumstances, a blank region in the lower thoracic segments might be observed (Fig. 3). Underestimation of CT attenuation coefficients results in an underestimation of SUV. Numerous methods have been

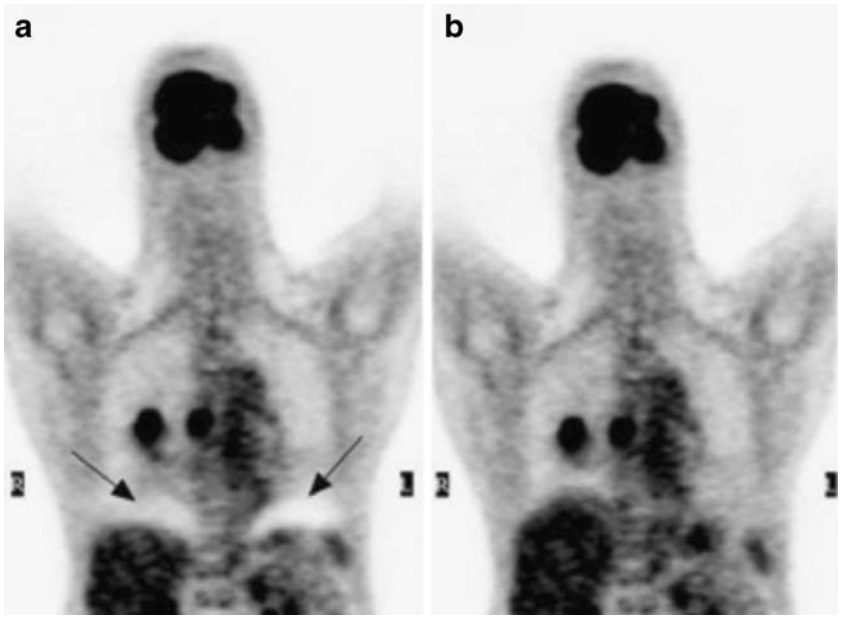

Fig. 3 Below-thoracic misregistration. Significant blank areas below the diaphragm are evident on the PET image with attenuation correction by HCT (**a** *arrows*). The artefact is almost completely corrected by attenuation correction by ACT (**b**)

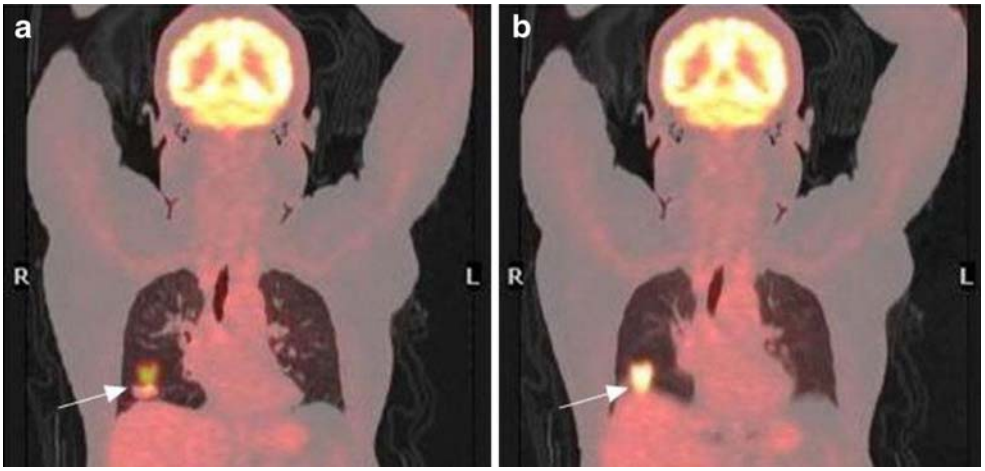

Fig. 4 Prominent misregistration. A 66-year-old male patient underwent a PET/CT scan for restaging of squamous cell lung carcinoma of the right lower lobe. Prominent misalignment of the image is apparent in the PET/HCT image (**a**) but this is corrected in the PET/ACT image (**b**). The tumour SUV_{max} in PET/HCT image was 7.4 (**a**) and 10.8 in PET/ACT (**b**)

developed to overcome the respiratory motion artefact [28]. In this study, we demonstrated the ability of PET/ACT to reduce the number of problematic locations in PET/HCT. Notably, the incidence of problematic locations in our study was similar to that reported by Osman et al. [17].

For evaluation of misregistration of PET and CT, lesion misregistration was added to below-thoracic misregistration since below-thoracic misregistration provided only indirect information about the artefact in the lower chest area and the correlation between lesion misregistration and change in SUV_{max} was highly significant. Misregistration (either below-thoracic misregistration or lesion misregistration) in ACT attenuation-corrected PET was significantly lower than in HCT attenuation-corrected PET among our NSCLC patients. One patient in this study showed moderate misregistration in PET/HCT, whereas PET/ACT provided better image registration (Fig. 4). An elevation in SUV_{max} up to 45.95% (from 7.4 in PET/HCT to 10.8 in PET/ACT) was evident.

Expert physicians may correct visually for misregistration between PET and CT. However, it is almost impossible to correct SUV_{max} by visual interpretation when misregistration exists. We found that SUV_{max} in ACT attenuation-corrected PET images were significantly higher than those obtained in HCT attenuation-corrected images both in primary tumours and regional lymph nodes (Tables 2 and 3). The elevation in SUV_{max} was most evident in primary tumours located in the lower lobe. Accordingly these lesions were closer to the diaphragm and had a higher probability of being corrected by ACT, thereby causing a greater elevation of SUV_{max}. In contrast, elevation of SUV_{max} for tumours in the middle lobe of the lung was not significant (p=0.198). Possible explanations for this apparent discrepancy could be the relatively central location of the middle lobe and the proximity to the heart that restrict respiratory motion. The limited number of patients (n=14) should be also considered.

Concerning lymph node lesions, a higher elevation of SUV_{max} was evident in the superior mediastinum as well as in the aortic groups of lymph nodes. Respiratory motion is due to movement of the diaphragm and expansion of the chest wall. Movement of the diaphragm accounts for 75% of the change in intrathoracic volume during quiet inspiration. Due to the relatively small size of lymph node lesions, they are prone to be influenced by respiratory motion. We therefore hypothesize that lymph nodes in the upper portion of lung may be influenced more by the chest wall expansion than diaphragm movement. Further investigations are needed to shed more light on this issue.

There are several reasons which prompted us to select the background activity in the aortic arch. First, the selection area was within the ACT field (from the apex to the liver dome). Second, the background was less influenced by respiratory motion (distant from the diaphragm). Third, in the background area there was no malignant or lung inflammatory process (the lung parenchyma was excluded). Fourth, the background area was similar to the mediastinal tissue. Fifth, data obtained in the background area should be reproducible in both intra- and interobserver evaluations. Finally, to avoid the possibility of heterogeneous FDG accumulation in the spine/ribs due to bone metastasis, bone was not selected as background.

The difference of background activity between PET/ACT and PET/HCT images was not significant (n=80, 2.04±0.37 in PET/HCT images and 2.05±0.38 in PET/ACT images, p=0.462). This suggests that the increase in SUV_{max} in PET/ACT images may not be due to background radioactivity. In contrast, it may be due to reduced misregistration of PET and CT caused by respiration. The absence of a significant increase in SUV_{max} in the vertebral lesions – which are considered to be immobile during respiration – further strengthens our hypothesis.

Compared to the findings of published studies [18, 19], the mean magnitude of elevation of SUV_{max} in PET/ACT images was much lower in our study. It is possible that the low body weight and height of our patients (57.3 kg and 1.60 m, respectively) could have resulted in a reduced

magnitude of respiratory motion. As a consequence, a reduced image misregistration and a smaller SUV change in PET/HCT and PET/ACT images could have occurred.

In addition to reduce misregistration and more precise measurement of SUV_{max}, based on our experience, we believe that ACT may be actually more convenient and cost-effective than other methods for suppressing respiratory motion. This may be especially true for a heavily loaded hospital such as ours. ACT does not require the use of a respiratory monitor or special software for complex postprocessing analysis. It is also worth noting that prescan and during-scan breathing coaching for respiratory control is not needed. All patients were free breathing for the entire examination. Besides these advantages, our results demonstrate that ACT may actually reduce the magnitude of misregistration, albeit not to zero.

It could be argued that the use of ACT attenuation-corrected PET would increase radiation burden in the chest region among NSCLC patients. In contrast with a total dose of 60 Gy or higher therapeutic doses given to NSCLC patients, in our current PET/CT protocol approximately 29.2 to 34.55 mSv were used. The dose derived from FDG (370 to 555 MBq) ranges between 10.7 and 16.05 mSv, whereas the dose derived from a CT scan (100 cm coverage) is 18.5 mSv. For patients weighing 70 kg or less, the addition of an ACT scan of 30 cm coverage is responsible for an additional dose of 2.5 mSv (or 5 mGy), that is 7.24% to 8.56% of a PET/CT dose [22]. Notably, the patients described here were treated with either curative intent radiotherapy (7 patients with stage I disease, Table 1) or concurrent chemoradiation therapy (70 patients with stage IIIa/IV disease). In comparison with the radiation dose from radiotherapy (total dose of 60 Gy or higher), the dose from ACT is unlikely to represent a major issue in this patient group. In contrast, ACT attenuation-corrected PET is not recommended as a routine diagnostic tool in healthy individuals, unless in the presence of suspect nodular lesions within the lung. Fortunately, it is possible to evaluate the patient data during the scan, as well as after HCT and PET. Thus additional ACT could be performed if misregistration of PET and CT data is severe. In this regard, we can decide whether we should perform ACT to save radiation dose as previously suggested [20].

In summary, we have provided evidence that the occurrence and magnitude of misregistration in ACT attenuation-corrected PET are significantly lower than in HCT attenuation-corrected PET. Significant elevations of SUV_{max} in primary tumours and lymph nodes were also observed. The use of ACT for attenuation correction of PET data may lead to more reliable measurements of SUV_{max}. It may thus prove useful in treatment planning and monitoring therapeutic responses in NSCLC patients.

Acknowledgments Averaged CT for attenuation correction of PET was originally developed by Dr. Tinsu Pan of the University of Texas, M.D. Anderson Cancer Center. We thank Dr. Pan for sharing his averaged CT software with us. Some of the results were presented at the Annual Meeting of SNM, 2008, in New Orleans, USA.

References

1. Shepherd FA, Rodrigues PJ, Ciuleanu T, et al. Erlotinib in previously treated non-small-cell lung cancer. N Engl J Med 2005;353:123–32.
2. Lilenbaum R, Axelrod R, Thomas S, et al. Randomized phase II trial of erlotinib or standard chemotherapy in patients with advanced non-small-cell lung cancer and a performance status of 2. J Clin Oncol 2008;26:863–9.
3. van Tinteren H, Hoekstra OS, Smit EF, et al. Effectiveness of positron emission tomography in the preoperative assessment of patients with suspected non-small-cell lung cancer: the PLUS multicentre randomised trial. Lancet 2002;359:1388–93.
4. Pieterman RM, van Putten JW, Meuzelaar JJ, et al. Preoperative staging of non-small-cell lung cancer with positron emission tomography. N Engl J Med 2000;343:254–61.
5. Eschmann SM, Friedel G, Paulsen F, et al. Repeat (18)F-FDG PET for monitoring neoadjuvant chemotherapy in patients with stage III non-small cell lung cancer. Lung Cancer 2007;55:165–71.
6. Yamamoto Y, Nishiyama Y, Monden T, et al. Correlation of FDG-PET findings with histopathology in the assessment of response to induction chemoradiotherapy in non-small cell lung cancer. Eur J Nucl Med Mol Imaging 2006;33:140–7.
7. Weber WA, Petersen V, Schmidt B, et al. Positron emission tomography in non-small-cell lung cancer: prediction of response to chemotherapy by quantitative assessment of glucose use. J Clin Oncol 2003;21:2651–7.
8. Choi NC, Fischman AJ, Niemierko A, et al. Dose-response relationship between probability of pathologic tumor control and glucose metabolic rate measured with FDG PET after preoperative chemoradiotherapy in locally advanced non-small-cell lung cancer. Int J Radiat Oncol Biol Phys 2002;54:1024–35.
9. MacManus MP, Hicks RJ, Matthews JP, et al. Metabolic (FDG-PET) response after radical radiotherapy/chemoradiotherapy for non-small cell lung cancer correlates with patterns of failure. Lung Cancer 2005;49:95–108.
10. MacManus MP, Hicks RJ, Matthews JP, et al. Positron emission tomography is superior to computed tomography scanning for response assessment after radical radiotherapy/chemoradiotherapy in patients with non-small-cell lung cancer. J Clin Oncol 2003;21:1285–92.
11. Eschmann SM, Friedel G, Paulsen F, et al. (18)F-FDG PET for assessment of therapy response and preoperative re-evaluation after neoadjuvant radio-chemotherapy in stage III non-small cell lung cancer. Eur J Nucl Med Mol Imaging 2007;34:463–71.
12. Hellwig D, Graeter TP, Ukena D, et al. Value of F-18-fluorodeoxyglucose positron emission tomography after induction therapy of locally advanced bronchogenic carcinoma. J Thorac Cardiovasc Surg 2004;128:892–9.
13. Kong FMS, Frey KA, Quint LE, et al. A pilot study of [^{18}F] Fluorodeoxyglucose positron emission tomography scans during and after radiation-based therapy in patients with non-small-cell lung cancer. J Clin Oncol 2007;25:3116–23.
14. Goerres GW, Burger C, Kamel E, et al. Respiration-induced attenuation artifact at PET/CT: technical considerations. Radiology 2003;226:906–10.

15. Goerres GW, Kamel E, Heidelberg TN, et al. PET-CT image co-registration in the thorax: influence of respiration. Eur J Nucl Med Mol Imaging 2002;29:351–60.
16. Cohade C, Osman M, Marshall LN, et al. PET-CT: accuracy of PET and CT spatial registration of lung lesions. Eur J Nucl Med Mol Imaging 2003;30:721–6.
17. Osman MM, Cohade C, Nakamoto Y, et al. Clinically significant inaccurate localization of lesions with PET/CT: frequency in 300 patients. J Nucl Med 2003;44:240–3.
18. Erdi YE, Nehmeh SA, Pan T, et al. The CT motion quantitation of lung lesions and its impact on PET-measured SUVs. J Nucl Med 2004;45:1287–92.
19. Pan T, Mawiawi O, Nehmeh SA, et al. Attenuation correction of PET images with respiration-averaged CT images in PET/CT. J Nucl Med 2005;46:1481–7.
20. Nehmeh SA, Erdi YE, Pan T, et al. Quantitation of respiratory motion during 4D-PET/CT acquisition. Med Phys 2004;31:1333–8.
21. Pan T, Lee TY, Rietzel E, Chen GTY. 4D-CT imaging of a volume influenced by respiratory motion on multi-slice CT. Med Phys 2004;31:333–40.
22. Pan T, Mawlawi O, Luo D, Liu HH, et al. Attenuation correction of PET cardiac data with low-dose average CT in PET/CT. Med Phys 2006;33:3931–8.
23. Gould KL, Pan T, Loghin C, Johnson NP, Guha A, Sdringola S. Frequent diagnostic errors in cardiac PET/CT due to misregistration of CT attenuation and emission PET images: a definitive analysis of causes, consequences, and corrections. J Nucl Med 2007;48:1112–21.
24. Alessio AM, Kohlmyer S, Branch K, Chen G, Caldwell J, Kinahan P. Cine CT for attenuation correction in cardiac PET/CT. J Nucl Med 2007;48:794–801.
25. Cook RA, Carnes G, Lee TY, Wells RG. Respiration-averaged CT for attenuation correction in canine cardiac PET/CT. J Nucl Med 2007;48:811–8.
26. Chi PC, Mawlawi O, Nehmeh SA, et al. Design of respiration averaged CT for attenuation correction of the PET data from PET/CT. Med Phys 2007;34:2039–47.
27. Mountain CF, Dresler CM. Regional lymph node classification for lung cancer staging. Chest 1997;111:1718–23.
28. Nehmeh SA, Erdi YE. Respiratory motion in positron emission tomography/computed tomography: a review. Semin Nucl Med 2008;38:167–76.